Journal of Alloys and Compounds 491 (2010) 747–752

Contents lists available at ScienceDirect

Journal of Alloys and Compounds

journal homepage: www.elsevier.com/locate/jallcom

Determination of the thermodynamic stability of TiB_2

Ashish Jain[a], R. Pankajavalli[a], S. Anthonysamy[a,*], K. Ananthasivan[a], R. Babu[a], V. Ganesan[a], G.S. Gupta[b]

[a] Chemistry Group, Indira Gandhi Centre for Atomic Research, Kalpakkam - 603 102, India
[b] Dept. of Materials Engineering, Indian Institute of Science, Banglore - 560 012, India

ARTICLE INFO

Article history:
Received 26 June 2009
Received in revised form 9 November 2009
Accepted 10 November 2009
Available online 14 November 2009

Keywords:
Titanium boride
Yttria doped thoria
EMF method
Standard free energy of formation
Enthalpy increment

ABSTRACT

The standard free energy of formation of titanium boride (TiB_2) was measured by the Electro Motive Force (EMF) method (by using yttria doped thoria (YDT) as the solid electrolyte). Two galvanic cells viz. Cell (I): Pt, TiB_2 (s), TiO_2 (s), B (s) |YDT| NiO (s), Ni (s), Pt and cell (II): Pt, TiB_2 (s), TiO_2 (s), B (s) |YDT| FeO (s), Fe (s), Pt were constructed in order to determine the $\Delta_f G^\circ$ of TiB_2. Enthalpy increments on TiB_2 were measured by using inverse drop calorimetry over the temperature range 583–1769 K. The heat capacity, entropy and the free energy function have been derived from these experimental data in the temperature range 298–1800 K. The mean value of the standard enthalpy of formation of TiB_2 ($\Delta_f H^\circ_{298}$ $\langle TiB_2 \rangle$) was obtained by combining these $\Delta_f G^\circ$ values and the free energy functions of TiB_2 derived from the drop calorimetry data. The mean values of $\Delta_f H^\circ_{298}$ $\langle TiB_2 \rangle$ derived from the $\Delta_f G^\circ$ data obtained from cell I and II were -322 ± 1.2 kJ mol^{-1} and -323.3 ± 2.1 kJ mol^{-1}, respectively. These values were found to be in very good agreement with the assessed data.

1. Introduction

TiB_2 is a refractory intermetallic compound with high hardness, low density, high electrical conductivity, good thermal shock resistance, chemical inertness, excellent wear and corrosion resistance and high elastic modulus [1,2]. These properties render it suitable for many applications, such as in the manufacture of wear resistant parts, ballistic armour, cathodes and thermocouple sheaths, crucibles for molten metals, metal evaporation boats and cutting tools as well as in tribological applications [2–7]. The neutron absorption properties of ^{10}B coupled with the high temperature stability of TiB_2 (containing ^{10}B) makes it a candidate material for the manufacture of the control rods for fast breeder reactors [8–10].

In the recent past many authors have reported the synthesis of TiB_2 and the composites of TiB_2 with $TiSi_2$ [11], TiC [12,13], ZrO_2 [14], B_4C [15,16], TiN [17], TiAl [18]. Advanced methods of synthesis such as electrochemical deposition [19], spark plasma sintering, combustion synthesis [20,21], sol–gel process and mechanical milling [22] have been used to synthesize TiB_2 and its composites. The magnetic [23] microstructural, thermal, electrical, electronic properties as well as bonding properties of TiB_2 [24] were also studied. Witusiewicz et al. [25] have reassessed the phase diagram of the system Ti–B by using the CALPHAD method and by incorporating more recent experimental data.

Fundamental thermodynamic quantities such as the enthalpy of formation at 298 K, entropy and heat capacity are required in order to estimate the standard free energy of formation of TiB_2. Several investigators have reported the standard enthalpy of formation of TiB_2 at 298 K ($\Delta_f H^\circ_{298}$ $\langle TiB_2 \rangle$) derived from different techniques, viz. equilibrium measurements [8,26–28], calorimetry [29–32] and vapour pressure techniques [33–36]. There is a large spread in these values (as large as ~190 kJ mol^{-1}). Moreover, there are discrepancies in the value of $\Delta_f H_{298^\circ}$ $\langle TiB_2 \rangle$ cited in the compendia on thermodynamic data [37,38]. The $\Delta_f H^\circ_{298}$ value of -280 kJ mol^{-1} cited in Ref. [37] and that compiled by Hultgren et al. [39] differ widely from the value of -316 kJ mol^{-1} suggested in Ref. [38].

The standard free energy of formation of TiB_2 has not been experimentally measured, although the estimated data have been reported in Refs. [37,38]. Even these estimates show significant scatter, possibly due to the uncertainties in the $\Delta_f H^\circ_{298}$ used in deriving them. Hence, in the present study, the free energy of formation of TiB_2 was determined from the EMF values obtained by using a galvanic cell that employed YDT as the solid electrolyte and a mixture of Ni, NiO (or Fe, FeO) as the reference electrode.

Enthalpy increments with TiB_2 were measured by using inverse drop calorimetry in the temperature range 583–1769 K. These were fitted into a polynomial equation which in turn was used to derive the temperature dependence of heat capacity, entropy and the free energy function. These results are presented and compared with the data cited in the literature.

---

* Corresponding author at: Dept. of Atomic Energy, Indira Gandhi Centre for Atomic Research, Kalpakkam - 603 102, India. Tel.: +91 44 27480500/24149; fax: +91 44 27480065.
E-mail address: sas@igcar.gov.in (S. Anthonysamy).

0925-8388/$ – see front matter © 2009 Elsevier B.V. All rights reserved.
doi:10.1016/j.jallcom.2009.11.058

The enthalpy of formation of TiB_2 was calculated by the 'third-law' method by using the free energy functions and the free energy of formation obtained in this study.

2. Experimental

Boron powder with a purity of 99.999% and NiO, FeO and TiO_2 with a purity >99% were procured from M/s. Aldrich, USA. A YDT solid electrolyte cup (10 mm dia and 2 mm tall) was obtained by cutting an YDT tube procured from M/s. Corning Inc., USA. Titanium boride was obtained from the Materials Processing Division (MPD), Bhabha Atomic Research Centre (BARC), Mumbai.

2.1. *Chemical purity of the starting material and phase equilibrium studies*

In order to ascertain the chemical purity of TiB_2 a complete chemical assay of TiB_2 was carried out with the help of an Inductively Coupled Plasma Mass Spectrometer (ICPMS, Model: Elan 250, M/s. Sciex, Toronto, Canada). X-ray diffraction analysis of TiB_2 was carried out by using an EXPERT MPD system supplied by M/s. Philips, The Netherlands.

The test electrode was a mixture of TiB_2, TiO_2 and B. It was prepared by homogenizing an equimolar mixture of the powdered constituents and cold compacting them in to pellets of 10 mm diameter and 1–2 mm height at a pressure of 100 MPa. These pellets were heat treated under helium at 900 K for 24 h. The phase purity of a heat treated pellet was ascertained by XRD analysis and it was found to contain only TiB_2, TiO_2 and B. These pellets were used as the test electrode in the EMF experiment.

2.2. *EMF measurements*

Electromotive Force (EMF) is by definition, the potential difference (voltage) across the two electrodes of a galvanic cell under open circuit conditions. This technique facilitates the measurement of thermodynamic properties with a higher degree of precision as compared to the other experimental methods. In the present study the attainment of thermodynamic equilibrium was ascertained by the constancy of the EMF. An accurate and precise measurement of the EMF was made possible by using a high impedance multimeter, Solartron 7150 supplied by M/s. Schlumberger Electronics (UK) Ltd., UK.

The cells of the following configurations were assembled for the present study:

$\mathrm{Pt, TiB_2(s), TiO_2(s), B(s)||YDT||NiO(s), Ni(s), Pt}$ (cellI)

$\mathrm{Pt, TiB_2(s), TiO_2(s), B(s)||YDT||FeO(s), Fe(s), Pt}$ (cellII)

where YDT represents a 7 wt% yttria doped thoria cup.

An open stacked pellet cell assembly as shown in Fig. 1 was used for the experiment. The sample and the reference electrodes were kept in good physical contact by pressing them against the surface of the YDT cup. In order to ensure that these electrodes were in good electrical contact with the respective leads, a platinum disc that was spot welded to the latter was placed on the pellets that constituted the electrodes. The platinum lead from the electrode at the top along with a Pt–10% Rh wire encased in a twin bore alumina sheath sealed together by means of Torr seal (M/s. Inland vacuum industries INC, New York) served as the thermocouple (Type S). The platinum lead from the electrode at the bottom was routed through a fine insulating capillary. Three stainless steel extension springs were employed in order to hold this stacked pellet assembly tightly through an intermediate quartz tube. The thermocouple (Type S) was calibrated at the freezing points of Sn, Zn, Sb and Ag as per ITS-90. The hot junction of the thermocouple was positioned in the uniform temperature zone of the furnace. The reproducibility of the EMF measurements was established not only by varying the mole ratios of the components of the reference and test electrodes, but also by thermal cycling and internal consistency checks. All other experimental details are the same as described elsewhere [40,41].

2.3. *Enthalpy increments measured with TiB_2 by drop calorimetry*

A "Multi-Detector" High Temperature Calorimeter (MHTC-96) with a drop detector of M/s. Setaram, France was employed for measuring the enthalpy increment on TiB_2. The tubular calorimetric detector consists of a thermopile having 36 thermocouples in which a sample crucible and an empty reference crucible are positioned one above the other. These thermocouples cover the whole surface enabling the measurement of an integrated heat exchange between the crucibles. In the present study, a drop detector, made up of Pt–30% Rh/Pt–6% Rh thermocouples was employed. This detector is placed in a gas-tight alumina tube which in turn is placed in the furnace heated by a graphite resistance heating element. In a typical experiment, five pairs of the samples of α-alumina reference (SRM 720) and TiB_2 pellets, each weighing about 150–200 mg, were placed in the individual slots of the specimen holder maintained at room temperature. The TiB_2 samples and the Al_2O_3 references were loaded in such a way that each sample was sandwiched between two Al_2O_3 references. The furnace was then gradually heated to the desired experimental temperature T under argon cover. Once the furnace attained the desired temperature the specimens were dropped alternatively from the specimen holder, into the sample crucible at the experimental temperature. From the resultant heat flow signals corresponding to the alumina reference and the TiB_2 sample, the enthalpy increments (TiB_2) were measured by using the critically assessed enthalpy increment values (alumina reference) reported in Ref. [42]. The mean of five such heat flow values for the standard and that for the sample were used to compute the enthalpy increment at that temperature. The experiment was repeated 4 or 5 times at the same temperature and the mean value of the enthalpy increments from these runs were taken for fitting. The calorimeter and the details of the experimental procedure have been described elsewhere [43].

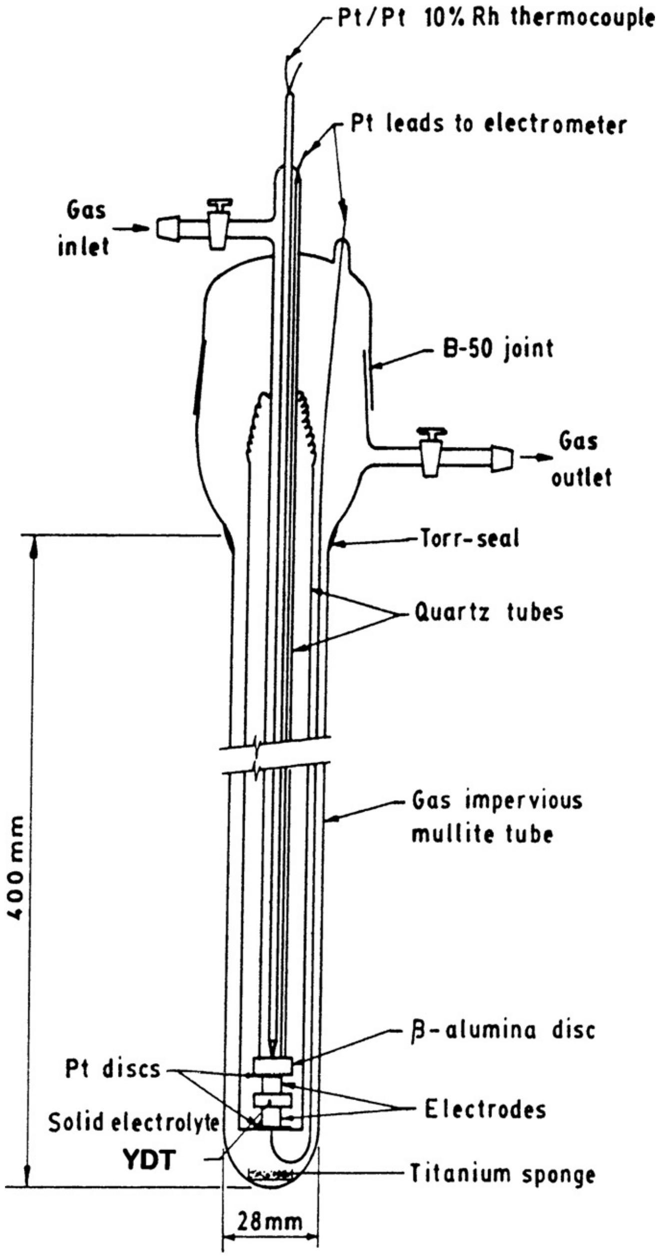

Fig. 1. Stacked pellets EMF cell assembly.

3. Results and discussion

3.1. *Purity of the starting material*

All the metallic impurities such as Fe and Ni that could affect the EMF measurement were found to be less than 100 ppm by weight. The X-ray diffraction pattern of TiB_2 is shown in Fig. 2. It was observed that all the peaks correspond to the standard pat-

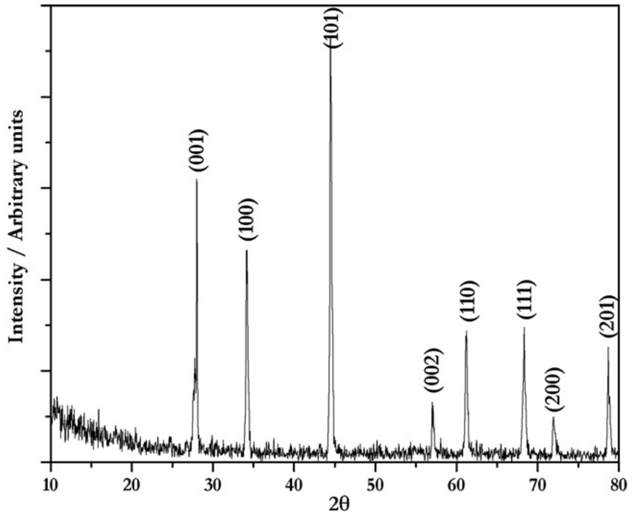

Fig. 2. X-ray diffraction pattern of TiB_2.

tern of TiB_2 (JCPDS file no. 85-2083). Further, measurement of the lattice parameter indicated that the sample is stoichiometric TiB_2. This observation is in agreement with the data reported by Murray et al. [44], Batzner [45] and Ma et al. [46] who considered TiB_2 as a stoichiometric compound up to its melting point.

3.2. *Free energy of formation of TiB_2*

The EMF values obtained by using the galvanic cells I and II are given in Tables 1 and 2, respectively. These data are also depicted in Figs. 3 and 4. A linear regression analysis of the experimental data yielded the following least-squares expressions, applicable over the temperature range of the actual measurements:

$$EMF_I = [338.6 + 0.0919T\,(K)] \pm 0.6\,(mV) \quad (887–1131\,K) \tag{1}$$

$$EMF_{II} = [71.3 + 0.1046T\,(K)] \pm 0.4\,(mV) \quad (832–1003\,K) \tag{2}$$

Table 1
Temperature dependence of EMF in cell I.

Cell I	
Temperature (K)	EMF (mV)
887	420
900	421.7
911	422.2
922	423.3
936	424.2
940	425
948	425.4
953	425.6
958	426.9
969	427.6
970	426.8
970	428.2
984	430.3
986	429.7
999	432
1016	433
1038	434
1051	435.5
1062	436.3
1074	437
1085	438
1100	439.5
1112	440.8
1124	442
1131	442.4

Table 2
Temperature dependence of the measured EMF of cell II.

Cell II	
Temperature (K)	EMF (mV)
999	165.7
1020	166.8
1039	167.2
1055	168.3
1075	169.5
1092	170.5
1115	172
1128	172.8

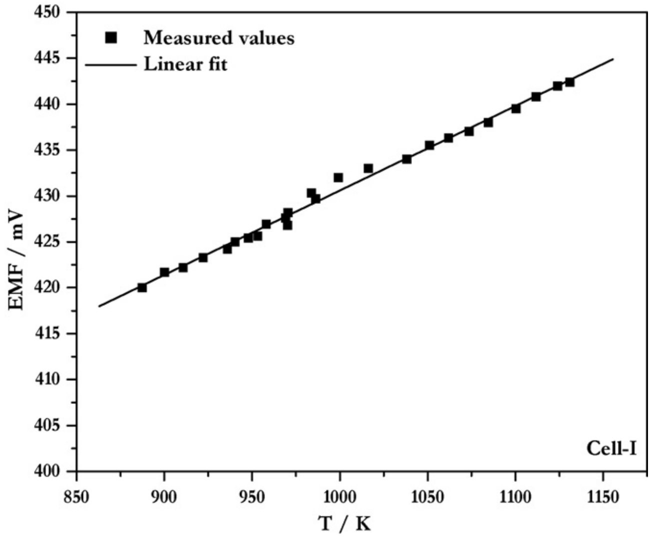

Fig. 3. Temperature dependence of EMF in cell I.

The two half-cell reactions of cell I are given by

$$TiB_2(s) + 2O^{2-} \rightarrow TiO_2(s) + 2B(s) + 4e^- \tag{3a}$$

$$2NiO(s) + 4e^- \rightarrow 2Ni(s) + 2O^{2-} \tag{3b}$$

For the passage of 4 Faraday of charge, the over-all chemical reaction could be represented by Eq. (4):

$$TiB_2(s) + 2NiO(s) \rightarrow TiO_2(s) + 2B(s) + 2Ni(s) \tag{4}$$

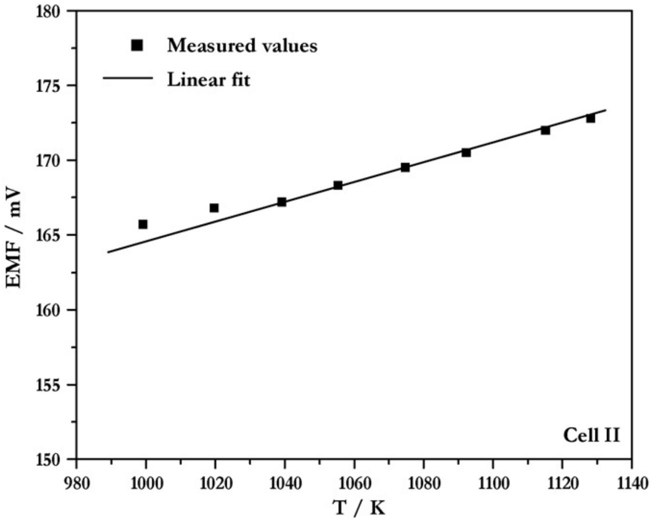

Fig. 4. Temperature dependence of EMF in cell II.

Table 3
Some thermodynamic functions of TiB_2.

T (K)	$H^\circ_T - H^\circ_{298}$ (kJ mol^{-1})		T (K)	$H^\circ_T - H^\circ_{298}$ (kJ mol^{-1})	C_p (J K^{-1} mol^{-1})	S°_T (J K^{-1} mol^{-1})	$-(G_T - H^\circ_{298})/T$ (J K^{-1} mol^{-1})
	Measured	Fit					
583	18.314	16.535	298	0	44.271	28.472	28.472
684	24.007	23.424	300	0.082	44.585	28.747	28.473
785	29.769	30.637	400	5.196	56.282	43.378	30.388
884	36.993	37.976	500	11.170	62.702	56.683	34.342
986	45.898	45.791	600	17.669	67.044	68.519	39.071
1086	54.241	53.684	700	24.547	70.406	79.115	44.048
1187	64.249	61.879	800	31.733	73.244	88.706	49.040
1287	69.110	70.205	900	39.186	75.779	97.482	53.942
1387	76.628	78.737	1000	46.882	78.125	105.589	58.706
1488	86.230	87.560	1100	54.807	80.348	113.140	63.315
1588	99.062	96.496	1200	62.949	82.487	120.223	67.766
1688	105.057	105.630	1300	71.302	84.566	126.908	72.060
1769	113.325	113.171	1400	79.861	86.603	133.250	76.206
–	–	–	1500	88.622	88.608	139.293	80.212
–	–	–	1600	97.582	90.588	145.075	84.087
–	–	–	1700	106.739	92.550	150.626	87.839
–	–	–	1800	116.091	94.498	155.971	91.476

The standard free energy change, $\Delta_r G^\circ_{(4)}$ of the above reaction is calculated by using the Nernst relation,

$$\Delta_r G^\circ_{(4)} = -4FE \qquad (5)$$

$$\Delta_r G^\circ_{(4)} = [-130.7 - 0.0355T\,(\mathrm{K})] \pm 0.2\,(\mathrm{kJ\,mol^{-1}}) \qquad (6)$$

where $\Delta_r G^\circ_{(4)}$ is the change in standard free energy for the reaction, F is the Faraday's constant and E is the EMF of the cell.

By combining Eq. (6) with the auxiliary data on the free energy of formation of TiO_2 [38] and NiO [38], an expression for the standard free energy of formation of TiB_2 was obtained (Eq. (7)):

$$\Delta_f G\circ < \mathrm{TiB_2} > = [-340.4 + 0.0414T\,(\mathrm{K})] \pm 2.2\,(\mathrm{kJ\,mol^{-1}}) \times (887\text{–}1131\,\mathrm{K}) \qquad (7)$$

The two half-cell reactions pertaining to cell II could be represented as follows:

$$\mathrm{TiB_2(s)} + 2\mathrm{O^{2-}} \rightarrow \mathrm{TiO_2(s)} + 2\mathrm{B(s)} + 4\mathrm{e^-} \qquad (8a)$$

$$2\mathrm{FeO(s)} + 4\mathrm{e^-} \rightarrow 2\mathrm{Fe(s)} + 2\mathrm{O^{2-}} \qquad (8b)$$

For the passage of 4 Faraday of charge, the over-all chemical reaction could be represented by

$$\mathrm{TiB_2(s)} + 2\mathrm{FeO(s)} \rightarrow \mathrm{TiO_2(s)} + 2\mathrm{B(s)} + 2\mathrm{Fe(s)} \qquad (9)$$

The $\Delta_r G^\circ_{(9)}$ of this reaction was found to be

$$\Delta_r G^\circ_{(9)} = [-27.5 - 0.0403T\,(\mathrm{K})] \pm 0.2\,(\mathrm{kJ\,mol^{-1}}) \qquad (10)$$

Combining the above expression (Eq. (10)) with the molar free energies of formation of FeO [47] and TiO_2, an expression for the molar free energy of formation of TiB_2 was calculated to be:

$$\Delta_f G\circ < \mathrm{TiB_2} > = [-389.6 + 0.0902T\,(\mathrm{K})] \pm 2.5\,(\mathrm{kJ\,mol^{-1}}) \times (832\text{–}1003\,\mathrm{K}) \qquad (11)$$

Eq. (7) was derived from as many as 25 measurements obtained by using the cell I in the temperature range 887–1131 K, while Eq. (11) was obtained from 8 measurements by using cell II in the temperature range 832–1003 K. Values obtained by using the cell II were used to validate the results obtained from cell I. The values of −299 kJ mol^{-1} and −299.4 kJ mol^{-1} at 1000 K for the free energy derived from these two independent measurements are in excellent agreement with each other and with the value of −300.6 kJ mol^{-1} cited in Ref. [38], while the values cited in Ref. [22] are higher (−264.2 kJ mol^{-1}).

3.3. Enthalpy increments by drop calorimetry

The enthalpy increment values measured in the temperature range of 583–1769 K were fitted in to a 4-term polynomial function using the least-squares method:

$$H_T - H^\circ_{298}/(\mathrm{J\,mol^{-1}}) = 61.427(T/\mathrm{K}) + 9.360 \times 10^{-3}(T/\mathrm{K})^2 + 20.212 \times 10^5(K/T) - 25,926 \qquad (12)$$

The following constraints were used for fitting the data: (a) $H_T - H^\circ_{298} = 0$ at 298 K and (b) the first derivative of this expression with respect to temperature at 298 K is equal to the value of heat capacity of TiB_2 at 298 K. The standard error in the fit was 3% and the standard deviation of the fit was estimated to be 1.7 kJ mol^{-1}. The experimentally measured enthalpy increment and the data obtained from the fit are given in Table 3. The s°_{298} value needed for the computation of the entropy and free energy functions were obtained from Ref. [9]. In addition, the calculated heat capacity, entropy and free energy functions at suitable temperature intervals (100 K) are also given in Table 3.

In Fig. 5, the measured and the fit values of enthalpy increments obtained from the present study are compared with the values given in Ref. [37]. It is seen that these two are in good agreement (within 1.7%). It is evident from Fig. 6 that the heat capacity values obtained in this study agree with those cited in Ref. [37]. The agreement between the present heat capacity is within 2% at temperatures below 1600 K and within 3% at temperatures above 1600 K, respectively.

3.4. Errors in EMF measurement

The EMF data represented by Eqs. (1) and (2) are precise within 0.6 (mV) and 0.4 (mV), respectively. These values would introduce an error of ±0.2 kJ mol^{-1} in the $\Delta_r G^\circ$ values derived through Eqs. (6) and (10). Other possible uncertainties which will contribute to the over-all error in the calculation of standard free energy of formation of TiB_2 [±2.2 kJ mol^{-1} (Eq. (7)) and ±2.5 kJ mol^{-1} (Eq. (11))] are due to the errors in the free energy of formation of TiO_2, NiO and FeO obtained from Ref. [39].

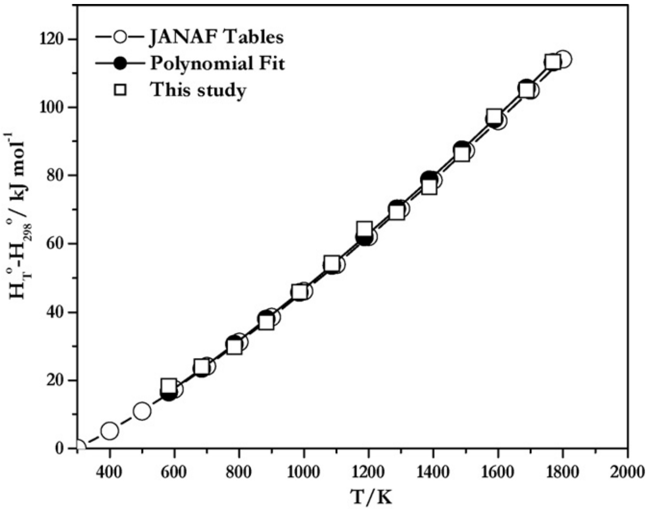

Fig. 5. Measured values of the enthalpy increments of TiB_2.

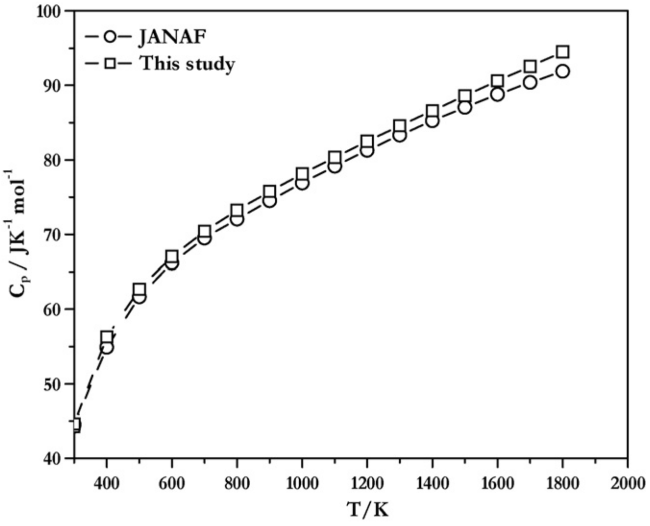

Fig. 6. Temperature dependence of C_p of TiB_2.

3.5. Third-law analysis of the EMF data

In order to examine if $\Delta_f G^\circ$ values obtained in this investigation are free from temperature dependent systematic errors, a "third-law" analysis [48] was carried out. This method verifies if the values of $\Delta_f H_{298}^\circ$ derived from the experimental data show any temperature dependence. This analysis is carried out by using the free energy functions (fef) cited in the literature. These (fefs) are auxiliary functions derived from independent experimental determinations. In this study the fef pertaining to various compounds involved in the equilibrium reactions were obtained from different standard compilations [37,38]. The 'fef' is defined as follows:

$$fef = \frac{G_T^\circ - H_{298}^\circ}{T} \tag{13}$$

where G_T° is the standard free energy of formation at temperature T, H_{298}° is the standard enthalpy at 298 K. The $\Delta_f H_{298}^\circ$ ⟨TiB_2⟩ value thus obtained was compared with the values cited in the literature (Table 4). Several investigators have experimentally determined the heat of formation of TiB_2 at 298 K [8,26–36]. The assessed values of $\Delta_f H_{298}^\circ$ are presented in Refs. [37,38] and are summarized in Table 4. Brewer and Haraldsen [26] have determined the thermodynamic stability of refractory borides by establishing an equilibrium between nitrogen and the boride phases. They found the value of $\Delta_f H_{298}^\circ$ ⟨TiB_2⟩ to be −301 kJ mol^{-1}, that was further confirmed by Samsonov [27]. However, the mass spectrometric studies by Schissel and Williams [33] yielded a value of −134 kJ mol^{-1} for $\Delta_f H_{298}^\circ$. The high temperature calorimetric measurement by Lowell and Williams [29] and the high temperature Knudsen effusion mass spectrometric studies by Schissel and Trulson [34] yielded $\Delta_f H_{298}^\circ$ ⟨TiB_2⟩ values of −209 kJ mol^{-1} and −218 kJ mol^{-1}, respectively. Williams [28] analyzed the above values [29,34] and recommended a value of −209 kJ mol^{-1}. Yurick and Spear [8] re-determined the enthalpy of formation of TiB_2 by an equilibrium study on the Ti–B–N system and obtained a value of −304 kJ mol^{-1} through a third-law analysis of their data. This value differs from the assessed values of −280 kJ mol^{-1} [37,39] and −316 kJ mol^{-1} [38]. The $\Delta_f H_{298}^\circ$ ⟨TiB_2⟩ value of about −280 kJ mol^{-1} presented in Ref [37] as well as by Hultgren et al. [39] were derived by assessing the calorimetric heats [29,30], vapour pressures [34–36] and equilibrium measurements involving TiB_2 [26–28]. Huber [31] performed oxygen bomb calorimetry of TiB_2 and reported a value of −324 kJ mol^{-1} for $\Delta_f H_{298}^\circ$ ⟨TiB_2⟩. Akhachinskij and Chirin [32] used the direct preparation of TiB_2 from its constituent elements in a Calvet calorimeter in order to derive a value of −319 kJ mol^{-1} for $\Delta_f H_{298}^\circ$ ⟨TiB_2⟩. Guzman et al. [49] quoted the value of −323.8 kJ mol^{-1} for $\Delta_f H_{298}^\circ$ ⟨TiB_2⟩.

In order to determine the value of $\Delta_f H_{298}^\circ$ ⟨TiB_2⟩ from the data obtained in this study, the free energy functions of TiB_2 were computed by combining the drop calorimetry data with the free energy functions of Ti and B obtained from Hultgren et al. [39]. The following reaction (14) was considered in the computation of this free

Table 4
Comparison of the values of $\Delta_f H_{298\circ}$ ⟨TiB_2⟩.

$\Delta_f G^\circ$ (kJ mol^{-1}) = (A + BT (K))		Temperature (K)	$\Delta_f H_{298}^\circ$ ⟨TiB_2⟩ (kJ mol^{-1})	References
A	B			
−340.4	0.0414	887–1131	−322.0	This study-cell I
−389.6	0.0902	832–1003	−323.3	This study-cell II
−317.3	0.0167	600–1100	−315.9	[38][a]
−280.9	0.0167	600–1100	−279.5	[37,39][a]
–		2270	−301.0	[26,27]
–		–	−134	[33]
–		1900–2250	−209	[28]
–		2100–2400	−218	[34]
–		–	−209	[29]
–		1850–2100	−304	[8]
–		–	−324	[3]
–		–	−319	[32]
–		–	−323.8	[49]

[a] Computed from the free energy data.

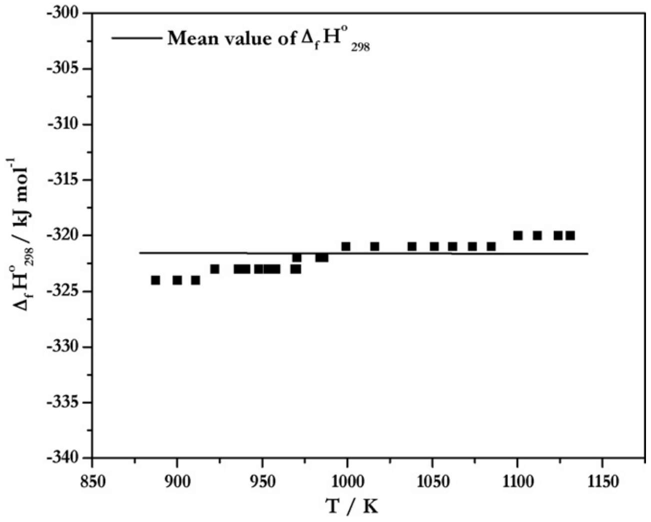

Fig. 7. Third-law analysis of the experimental (EMF) data.

energy function (Δfef):

$$\text{Ti(s)} + \text{2B(s)} \rightarrow \text{TiB}_2\text{(s)} \quad (14)$$

The values of $\Delta_r G^\circ_{(4)}$ and $\Delta_r G^\circ_{(9)}$ were computed for each experimental temperature using the EMF data listed in Tables 1 and 2. These free energy data were combined with the corresponding values of $\Delta_f G^\circ \langle \text{NiO} \rangle$ or ($\Delta_f G^\circ \langle \text{FeO} \rangle$) and $\Delta_f G^\circ \langle \text{TiO}_2 \rangle$ in order to derive $\Delta_f G^\circ \langle \text{TiB}_2 \rangle$ from cells I and II. The $\Delta_f H^\circ_{298} \langle \text{TiB}_2 \rangle$ value pertaining to each measurement was computed by using Eq. (15):

$$\Delta_f H^\circ_{298\text{K}}(\text{TiB}_2) = \Delta_f G^\circ(\text{TiB}_2) - T \times \Delta\text{fef} \quad (15)$$

The Δfef values interpolated at the actual temperature at which the EMF measurement was carried out were combined with the computed values of $\Delta_f G^\circ \langle \text{TiB}_2 \rangle$ in order to derive $\Delta_f H^\circ_{298} \langle \text{TiB}_2 \rangle$. A third-law plot of $\Delta_f H^\circ_{298} \langle \text{TiB}_2 \rangle$ (Fig. 7) indicates that our experimental measurements do not suffer from significant temperature dependent errors. The values of -322 ± 1.2 kJ mol^{-1} and -323.3 ± 2.1 kJ mol^{-1} were derived for $\Delta_f H^\circ_{298} \langle \text{TiB}_2 \rangle$ from cells I and II, respectively. The enthalpy of formation of TiB_2 at 298 K obtained from our measurements are in good agreement with the data reported in the standard reference [38] as well as with those reported by most of the investigators (Table 4).

4. Conclusions

The standard free energy of formation of TiB_2 was determined for the first time by using an EMF method that employed yttria doped thoria as the oxide solid electrolyte. Enthalpy increments of TiB_2 were measured by using inverse drop calorimetry over the temperature range 583–1769 K. By using the measured values of the enthalpy increments, other thermodynamic functions viz., heat capacity, entropy and the free energy function have been derived in the temperature range 298–1800 K. Two independent EMF measurements (cell I and cell II) carried out in this study yielded $\Delta_f H^\circ_{298}$ values of -322 ± 1.2 kJ mol^{-1} and -323.3 ± 2.1 kJ mol^{-1}, respectively. These values agree with those cited in the literature as well.

Acknowledgements

The authors wish to thank Mr. C. Subramanian, Materials Processing Division, Bhabha Atomic Research Centre, Mumbai for providing TiB_2 powder for this study. Authors are also grateful to Dr. K. Nagarajan, Chemistry Group, Indira Gandhi Centre for Atomic Research, for providing support in the calorimetric measurements on the TiB_2 sample.

References

[1] R. Telle, G. Petzow, Mater. Sci. Eng. A 105–106 (1988) 97–104.
[2] U. Demircan, B. Derin, O. Yucel, Mater. Res. Bull. 42 (2007) 312–318.
[3] T.S.R.Ch. Murthy, B. Basu, A. Srivastava, R. Balasubramaniam, A.K. Suri, J. Eur. Ceram. Soc. 26 (2006) 187–192.
[4] C. Morz, D. Titanium, Am. Ceram. Soc. Bull. 74 (1995) 158–159.
[5] J.J. Gamgler, J. Am. Ceram. Soc. 33 (1950) 367–374.
[6] B. Basu, G.B. Raju, A.K. Suri, Int. Mater. Rev. 51 (2006) 352–372.
[7] J.J. Fang, Z.X. Li, Y.W. Shi, Appl. Surf. Sci. 254 (2008) 3849–3858.
[8] T.J. Yurick, K.E. Spear, Thermodynamics of TiB_2 from Ti–B–N studies, IAEA-SM-236/53, 1980, pp. 73–90.
[9] E.F. Westrum Jr., G.A. Clay, J. Chem. Thermodyn. 10 (1978) 629–636.
[10] C. Subramanian, T.S.R.Ch. Murthy, A.K. Suri, Int. J. Refract. Met. Hard Mater. 25 (2007) 345–350.
[11] T.S.R.Ch. Murthy, C. Subramanian, R.K. Fotedar, M.R. Gonal, P. Sengupta, S. Kumar, A.K. Suri, Int. J. Refract. Met. Hard Mater. 27 (2009) 629–636.
[12] D. Vallauri, I.C. Atías Adrián, A. Chrysanthou, J. Eur. Ceram. Soc. 28 (2008) 1697–1713.
[13] C.L. Yeh, Y.L. Chen, J. Alloys Compd. 463 (2008) 373–377.
[14] B. Basu, J. Vleugels, O. Van der Biest, J. Eur. Ceram. Soc. 25 (2005) 3629–3637.
[15] L.Z. Pei, H.N. Xiao, J. Mater. Process. Technol. 209 (2009) 2122–2127.
[16] H. Itoh, K. Sugiura, H. Iwahara, J. Alloys Compd. 232 (1996) 186–191.
[17] C.L. Yeh, G.S. Teng, J. Alloys Compd. 424 (2006) 152–158.
[18] C.L. Yeh, S.H. Su, J. Alloys Compd. 407 (2006) 150–156.
[19] U. Fastner, T. Steck, A. Pascual, G. Fafilek, G.E. Nauer, J. Alloys Compd. 452 (2008) 32–35.
[20] L. Zhan, P. Shen, S. Jin, Q. Jiang, J. Alloys Compd. 480 (2009) 315–320.
[21] Z.I. Zaki, E.M.M. Ewais, M.M. Rashad, J. Alloys Compd. 467 (2009) 288–292.
[22] A. Calka, D. Oleszak, J. Alloys Compd. 440 (2007) 346–348.
[23] G.E. Grechnev, A.V. Fedorchenko, A.V. Logosha, A.S. Panfilov, I.V. Svechkarev, V.B. Filippov, A.B. Lyashchenko, A.V. Evdokimova, J. Alloys Compd. 481 (2009) 75–80.
[24] Y. Han, Y. Dai, D. Shu, J. Wang, B. Sun, J. Alloys Compd. 438 (2007) 327–331.
[25] V.T. Witusiewicz, A.A. Bondar, U. Hecht, S. Rex, T.Ya. Velikanova, J. Alloys Compd. 448 (2008) 185–194.
[26] L. Brewer, H. Haraldsen, J. Electrochem. Soc. 102 (1955) 399–406.
[27] G.V. Samsonov, J. Appl. Chem. (USSR) 28 (1955) 975.
[28] W.S. Williams, J. Phys. Chem. 65 (1961) 2213–2216.
[29] C.E. Lowell, W.S. Williams, Rev. Sci. Instrum. 32 (1961) 1120–1123.
[30] V.A. Epel'baum, M.L. Starostina, Bor. Trudy Konf. Khim., Bora i Ego Soedinenii. (1958) 97.
[31] E.J. Huber Jr., J. Chem. Eng. Data 11 (1966) 430–431.
[32] V.V. Akhachinskij, N.A. Chirin, Proceeding of Symposium on Thermodynamics of Nuclear Materials, Vol. 2, IAEA, Vienna, 1975, pp. 467–472.
[33] P.O. Schissel, W.S. Williams, Bull. Am. Phys. Soc. Ser. II 4 (3) (1959).
[34] P.O. Schissel, O.C. Trulson, J. Phys. Chem. 66 (1962) 1492–1496.
[35] G.M. Kibler, T.F. Lyon, M.J. Linevsky, V.J. Desantis, Technical Report No. WADD-TR-60-646. Part III, vol. 2, General Electric Co., Evandale, OH, 1964.
[36] V.V. Fesenko, A.S. Bolgar, Sov. Powder Metall. Met. Ceram. 1 (1963) 11–15.
[37] M.W. Chase Jr., C.A. Davis, J. Downey Jr., D.J. Frurip, R.A. Mcdonald, A.N. Syveud, JANAF Thermochemical Tables, III ed., 1985, pp. 274–275.
[38] O. Knacke, O. Kubaschewski, K. Hesselmann (Eds.), Thermochemical Properties of Inorganic Substances, second ed., Springer–Verlag, Germany, 1991.
[39] R. Hultgren, P.D. Desai, D.T. Hawkins, M. Gleiser, K.K. Kelley, Selected Values of the Thermodynamic Properties of Binary Alloys, American Society for Metals, Metals Park, OH, 1973, pp. 516–521.
[40] A.M. Azad, O.M. Sreedharan, J. Appl. Electrochem. 17 (1987) 949–955.
[41] R. Pankajavalli, K. Ananthasivan, S. Anthonysamy, P.R. Vasudeva Rao, J. Nucl. Mater. 336 (2005) 177–184.
[42] Synthetic Sapphire Al_2O_3, Certificate of Standard Reference Materials, SRM 720, National Bureau of Standards, U.S. Department of Commerce, Washington, DC, USA, 1982.
[43] R. Kandan, R. Babu, P. Manikandan, R. Venkata Krishnan, K. Nagarajan, J. Nucl. Mater. 384 (2009) 231–235.
[44] J.L. Murray, P.K. Liao, K.E. Spear, in: J.L. Murray (Ed.), Phase Diagrams of Binary Titanium Alloys, ASM International, Materials Park, OH, 1987, pp. 33–38.
[45] C. Batzner, 'System B-Ti', COST507, in: I. Ansara, A.T. Disdale, M.H. Rand (Eds.), Thermochemical Database for Light Metal Alloys, European Commission, Luxembourg, 1998.
[46] X. Ma, C. Li, Z. Du, W. Zhang, J. Alloys Compd. 370 (2004) 149–158.
[47] O.M. Sreedharan, C. Mallika, A Compilation of Gibbs Energy Data for 40 Metal Oxide Buffers, Report RRC – 69, 1984, pp. 1–34.
[48] O. Kubaschewskii, High Temp. High Pressure 4 (1972) 1–5.
[49] L. Guzman, M. Elena, A. Miotello, P.M. Ossi, D.C. Kothari, Vacuum 46 (1995) 951–954.